ELSEVIER

Biophysical Chemistry 78 (1999) 207–217

Biophysical Chemistry

Heat capacity and compactness of denatured proteins

Themis Lazaridis[a,*,1], Martin Karplus[a,b,*]

[a] *Department of Chemistry and Chemical Biology, Harvard University, Cambridge, MA 02138, USA*
[b] *Laboratoire de Chimie Biophysique, ISIS, Université Louis Pasteur, 67000 Strasbourg, France*

Received 6 November 1998; received in revised form 2 February 1999; accepted 10 February 1999

Abstract

One of the striking results of protein thermodynamics is that the heat capacity change upon denaturation is large and positive. This change is generally ascribed to the exposure of non-polar groups to water on denaturation, in analogy to the large heat capacity change for the transfer of small non-polar molecules from hydrocarbons to water. Calculations of the heat capacity based on the exposed surface area of the completely unfolded denatured state give good agreement with experimental data. This result is difficult to reconcile with evidence that the heat denatured state in the absence of denaturants is reasonably compact. In this work, sample conformations for the denatured state of truncated CI2 are obtained by use of an effective energy function for proteins in solution. The energy function gives denatured conformations that are compact with radii of gyration that are slightly larger than that of the native state. The model is used to estimate the heat capacity, as well as that of the native state, at 300 and 350 K via finite enthalpy differences. The calculations show that the heat capacity of denaturation can have large positive contributions from non-covalent intraprotein interactions because these interactions change more with temperature in non-native conformations than in the native state. Including this contribution, which has been neglected in empirical surface area models, leads to heat capacities of unfolding for compact denatured states that are consistent with the experimental heat capacity data. Estimates of the stability curve of CI2 made with the effective energy function support the present model.

Keywords: Protein thermodynamics; Solvent effects; Non-bonded interactions; Stability of proteins

* Corresponding authors.
[1] Present address: Department of Chemistry, City College of New York, Convent Ave and 138th St., New York, NY 10031, USA.

0301-4622/99/$ - see front matter
PII: S0301-4622(99)00022-8

1. Introduction

One of the fundamental quantities in protein thermodynamics is the partial molar heat capacity change, $\Delta^D_N \overline{C}_p$, associated with the unfolding reaction. The non-zero values of $\Delta^D_N \overline{C}_p$ lead to the curvature of the stability curve (free energy of unfolding as a function of temperature) and are linked to important phenomena, including hyperthermostability and cold denaturation. Since $\Delta^D_N \overline{C}_p$ can be measured by calorimetry and has been determined for many proteins, to understand its origin is of particular interest. Measurements show $\Delta^D_N \overline{C}_p$ is typically of the order of 12–20 cal/mol K per residue [1]. The partial molar heat capacity of native proteins increases linearly with temperature whereas the partial molar heat capacity of the denatured state is somewhat non-linear, tending to level off at high temperatures [2]. As a result, $\Delta^D_N \overline{C}_p$ varies with temperature, has a maximum near room temperature, and decreases at lower and higher temperatures [1].

It is generally believed that the positive $\Delta^D_N \overline{C}_p$ values arise primarily from the exposure of non-polar groups to water [3–8]. The basis for this conclusion is that the transfer of non-polar groups from the gas phase or non-polar liquids into water is also accompanied by a large positive heat capacity change [9]. More recently, it was realized that polar groups also make a contribution to $\Delta^D_N \overline{C}_p$ that is smaller and of the opposite sign to that of non-polar groups [6,10,11]. It has been found that $\Delta^D_N \overline{C}_p$ can be well reproduced assuming a fully unfolded denatured state (all residues fully exposed to solvent [2]) if $\Delta^D_N \overline{C}_p$ is taken to be proportional to the change in the exposed surface area on unfolding. In such calculations the proportionality constants appropriate for the amino acids are obtained from small model compound transfer experiments [6,11–13].

Such a fully unfolded thermally induced denatured state is difficult to reconcile with other experimental evidence showing that the denatured state in the absence of denaturants is rather compact on the average and includes populations ranging from highly compact to rather unfolded configurations of the polypeptide chain [14,15]. Already in the work of Tanford [16], it was shown that the heat denatured state is not as unfolded as the chemically denatured state. Recent solution X-ray scattering [17] and CD and FTIR [17–19] experiments on heat denatured ribonuclease A showed that this state is compact and contains significant amounts of 'residual structure', although it is not native-like because it does not offer significant protection from hydrogen exchange [20]. Residual structure has also been found in the heat denatured states of other proteins [21,22]. Experiments indicating that the denatured state is compact have been summarized by Shortle [23]. Theoretical work on simplified protein models [24,25] and molecular dynamics (MD) simulations in explicit solvent [26,27] also suggest a relatively compact denatured state. Residual structure and compactness implies that a large fraction of the protein residues are interacting with each other and are, at least in part, sequestered from solvent, although the fluctuations in the structures are such that little hydrogen exchange protection is present.

The experiments and simulation results on the compact nature of the denatured state appear inconsistent with the standard interpretation of $\Delta^D_N \overline{C}_p$ which assumes a fully unfolded state. To resolve this question we generalize a recently developed model (EEF1) that approximates the effective energy (potential of mean force) of proteins in solution [28,29] for the calculation of the partial molar heat capacity of polypeptides and proteins and show how to use this model to evaluate $\Delta^D_N \overline{C}_p$. The native state is obtained from the X-ray structure and the denatured state is generated by MD simulations. We use the same approach to estimate the stability curve, $\Delta^D_N G$ of unfolding, for both compact and extended models for the denatured state. The system we use to illustrate the approach is the 64-residue truncated version of the small protein CI2, for which experimental data and unfolding simulations are available.

2. Theory

The heat capacity of unfolding at constant pressure, as determined by calorimetric experi-

ments [30], is the difference in partial molar heat capacity between the native (N) and denatured (D) states and is equal to the temperature derivative of the enthalpy of unfolding (the corresponding difference in partial molar enthalpy); that is,

$$\Delta_N^D \overline{C}_p = \overline{C}_p^{(D)} - \overline{C}_p^{(N)} = \left(\frac{\partial \Delta_N^D \overline{h}}{\partial T} \right)_P \quad (1)$$

where the overbar denotes a partial molar property of the protein (the increment in that property when a mole of protein is added to the solution at constant temperature and pressure). For simplicity we omit the constant pressure subscript on the derivatives in what follows. For classical, non-polarizable Hamiltonians, such as those used in most molecular mechanics energy functions [31,32], and for sufficiently dilute solutions so that the protein molecules do not interact with each other, the partial molar enthalpy of the N or D state can be divided into two contributions: the partial molar enthalpy in an ideal gas (ig) state at the same temperature and density, and the excess partial molar enthalpy (or solvation enthalpy, the enthalpy change upon transfer of the protein from the gas phase to solution at constant T and P):

$$\overline{h}^{(K)} = \overline{h}^{ig,(K)} + \overline{h}^{ex,(K)}, \quad K = N \text{ or } D \quad (2)$$

The first term in the RHS contains the contribution from kinetic energy and from the intramolecular potential energy (the $P\bar{v} = RT$ term can be included with $\overline{h}^{ex}$ to bring it closer to Ben-Naim's standard solvation enthalpy [33]). The partial molar heat capacity can be written

$$\overline{C}_p^{(K)} = \frac{\partial \overline{h}^{ig,(K)}}{\partial T} + \frac{\partial \overline{h}^{ex,(K)}}{\partial T}, \quad K = N \text{ or } D \quad (3)$$

and the heat capacity of unfolding

$$\Delta_N^D \overline{C}_p = \frac{\partial \Delta_N^D \overline{h}^{ig}}{\partial T} + \frac{\partial \Delta_N^D \overline{h}^{ex,(K)}}{\partial T} \quad (4)$$

Theoretical calculation of the gas phase contribution in Eq. (3) can in principle be made with classical mechanics. However, many components of the intramolecular energy in proteins, such as bond stretching terms and to a smaller extent bond angle bending terms, are associated with high frequency vibrations, and their contributions to the heat capacity at room temperature are greatly overestimated by classical mechanics [34]. For example, the contribution of a typical protein bond to the heat capacity (frequency $\upsilon \approx 1240$ cm^{-1}), if viewed as an independent harmonic oscillator, is approximately 0.1 R at room temperature, whereas the classical harmonic oscillator gives R from the derivative of the potential and kinetic energy. On the other hand, the non-bonded interactions are associated with much lower frequencies and can be treated classically. For example, a typical Lennard–Jones interaction ($\upsilon \approx 36$ cm^{-1}, from a Taylor expansion of the potential around the minimum) gives ~ 0.998 R, essentially the classical limit. The alternative to classical mechanics is to perform a normal mode analysis, calculate the frequencies of all normal modes, and use the equations of a quantum mechanical harmonic oscillator to compute the thermodynamic properties [35,36]. However, this approach would not allow us to study the effects of large conformational fluctuations that are not described by the harmonic approximation and to separate out the contribution of non-bonded interactions.

In this work we follow the classical approach and make use of molecular dynamics but neglect the kinetic energy contribution. We also do not include the contribution of the non-polar hydrogens, which are not treated explicitly in CHARMM 19 and EEF1. This approach overestimates the contribution of stiff degrees of freedom and underestimates the contribution of soft degrees of freedom. The reasonable values for the partial molar heat capacities obtained by this method (see Section 4) must, therefore, result from a cancellation between the two types of errors. However, disregarding the fortuitous cancellation, it is the 'difference' in partial molar heat capacity between N and D which is of primary interest here. This is expected to be reliable in the classical limit because the kinetic energy contribution does not change and the quantum mechanical effects involving stiff bonds

are expected to be the same in N and D. In what follows we write

$$\frac{\partial \overline{h}^{ig,(K)}}{\partial T} \approx \frac{\partial E^{intra,(K)}}{\partial T}, \quad K = N \text{ or } D \tag{5}$$

where E^{intra} is the intramolecular potential energy, realizing that Eq. (5) is most accurate for the difference between N and D; i.e. for the calculation of $\Delta^D_N \overline{C}_p$ as in Eq. (1).

The various classical intramolecular terms in the energy function, such as the covalent (bond stretching and bending, etc.) and non-covalent (van der Waals and electrostatic) interactions, can be assumed to be approximately independent of temperature, so that E^{intra} varies with temperature primarily through the change in the distribution of conformations:

$$\left(\frac{\partial E^{intra,(K)}}{\partial T}\right)_{p(\mathbf{q})^{(K)}} = 0, \quad K = N \text{ or } D \tag{6}$$

where $\mathbf{q}$ is a set of variables describing the conformation of the protein and $p(\mathbf{q})^{(K)}$ is the conformational distribution of the protein in the state K. The solvation term in Eq. (4) has two contributions, one from the change in solvation enthalpy with temperature at constant $p(\mathbf{q})$, and another from the change in the distribution of conformations with temperature. Thus, the partial molar heat capacity of state K can be written:

$$\begin{aligned}\overline{C}_p^{(K)} = &\int \frac{\delta E^{intra,(K)}}{\delta p(\mathbf{q})^{(K)}} \frac{\partial p(\mathbf{q})^{(K)}}{\partial T} d\mathbf{q} \\ &+ \left(\frac{\partial \overline{h}^{ex,(K)}}{\partial T}\right)_{p(\mathbf{q})^{(K)}} \\ &+ \int \frac{\delta \overline{h}^{ex,(K)}}{\delta p(\mathbf{q})^{(K)}} \frac{\partial p(\mathbf{q})^{(K)}}{\partial T} dq, \quad K = N \text{ or } D\end{aligned} \tag{7}$$

where the derivatives with respect to $p(\mathbf{q})$ are functional derivatives [37].

Since the denatured state is a collection of basins (local minima) on the effective energy surface, its heat capacity will contain one contribution from the protein conformational relaxation within each basin and another from the redistribution of the protein population among the basins as the temperature is changed. In this work we calculate only the first contribution. Estimation of the second contribution requires sampling of a large number of denatured basins and calculation of how their statistical weights change with temperature [38–40]. The native state can be viewed as occupying a single basin on the effective energy hypersurface. Therefore, there is no summation over basins and no contribution to the heat capacity from redistribution among basins. Reasonable estimates of the thermodynamic properties of protein native states, including the heat capacity, can be made by use of the harmonic approximation [35], although multiple conformers of sidechains make a small additional contribution [41,42].

Empirical models for the calculation of the heat capacity account for the terms in Eq. (7) in different ways. Models which use data for the transfer of model compounds from non-polar liquids to water [8,11] implicitly account for the non-covalent contributions in the first term and for the second term; i.e. the interactions of the model compound in the non-polar liquid are assumed to mimic the interactions of similar groups in the protein interior. Most such models neglect the contribution of covalent intramolecular interactions to $\Delta^D_N \overline{C}_p$. Models which use data for the transfer of model compounds from the gas phase to water [1] estimate the second term based on accessible surface area and the first term by difference from the experimental value [1,7,43]; in the latter, a covalent contribution is included implicitly. Because all models to date use a single, fixed conformation as a description for the denatured state (a fully extended chain or the surface area of Gly–X–Gly tripeptides), none of them accounts for the last term in Eq. (7), which is due to changes in the conformational distribution of the denatured polypeptide chain.

3. Methods

In this paper we estimate $\Delta^D_N \overline{C}_p$ using Eq. (7) for N and D. We perform molecular dynamics

simulations at different temperatures and use the resulting structures to calculate the enthalpy [Eq. (1)] and estimate the various contributions to $\Delta_N^D \overline{C}_p$ by finite differences. The simulations are performed with the implicit solvent model embodied in EEF1 [29], a recently proposed effective energy function consisting of the CHARMM polar hydrogen energy function [32,44] and an implicit solvation term [28,29]. EEF1 has been shown to give stable native structures in room temperature MD simulation [29], reasonable energies for unfolded and misfolded conformations [29] and unfolding pathways in agreement with explicit water simulations [28]. As pointed out in [29], the same implicit solvation model can be used to calculate solvation enthalpies by substituting solvation enthalpy group contributions [45] for solvation free energy group contributions. The method was applied to estimate the unfolding enthalpy of helices [29].

To obtain models for the denatured state, we started from a fully extended chain and performed three simulations ($D1$, $D2$, $D3$) with different initial velocities. The simulations lasted 1.15 ns (100 ps at 600 K and 1050 ps at 300 K), during which the chain collapsed to a compact conformation. Starting from the three models obtained at the end of these simulations, we did 20-ps MD simulations at 280 and 320 K; the last 2 ps of the simulations were used for calculating averages. For $D1$ the simulations were extended to 50 ps and averaged over the last 6 ps; the results were very similar. The native protein was also subjected to 20-ps MD simulations at 280 and 320 K; these simulations started from an equilibrated structure of native CI2 after 50 ps of MD at 300 K. The contributions of internal (covalent and non-covalent) interactions and of solvation to the enthalpy are readily obtained from the simulations with the EEF1 model and enthalpy parameters. The group solvation free energies at temperatures other than 300 K are calculated from the experimental estimates of the group solvation enthalpies and heat capacities [29]. Temperature-independent group heat capacities at 298 K were used in this calculation [7].

The heat capacity was also estimated at 350 K. The native and the three denatured conformations were first simulated at 350 K for 50 ps. Each of the resulting structures was simulated at 330 and 370 K for 20 ps, as above, and the last 2 ps were used in calculating averages. This calculation accounts for the change in conformational distribution within individual basins on the effective energy hypersurface but not for the possible redistribution of the protein population among basins (see above). Thus, the calculation is expected to underestimate the heat capacity of the denatured state.

To provide an additional criterion for the validity of the model, we use it to estimate the stability of the protein as a function of temperature. The standard free energy of unfolding (the difference in the chemical potential of the denatured and native forms) is

$$\Delta G = \Delta\langle W\rangle - T\Delta S^{conf} = \Delta\langle E^{intra}\rangle + \Delta\langle \Delta G^{slv}\rangle - T\Delta S^{conf} \quad (8)$$

where $\Delta\langle W\rangle$ is the change in the average effective energy, $\Delta\langle \Delta G^{slv}\rangle$ is the change in the average solvation free energy and ΔS^{conf} is the change in conformational entropy upon unfolding. The value of W is obtained from EEF1 [29]. For the calculation we take $\Delta\langle E^{intra}\rangle$ and ΔS^{conf} to be independent of temperature. This is not strictly true, but the two terms compensate each other to a large extent in the free energy of unfolding (both increase with temperature). Consequently, the T factor in the conformational entropy term and the temperature dependence of the solvation free energy should yield a qualitatively correct stability curve with the present model. For each structure of the denatured state ($D1$, $D2$, $D3$ and completely extended, E), we calculate $\Delta\langle E^{intra}\rangle$ and $\Delta\langle \Delta G^{slv}\rangle$ at 300 K and determine ΔS^{conf} by fitting the experimental ΔG at that temperature; the value used (7 kcal/mol) is that given by Jackson and Fersht [46]. Then, we keep $\Delta\langle E^{intra}\rangle$ and ΔS^{conf} constant, as indicated above, and determine $\Delta\langle \Delta G^{slv}\rangle$ as a function of temperature from the implicit solvation model.

4. Results and discussion

All three simulations starting from the fully extended chain resulted in a relatively compact structure. The energetic and structural characteristics of the three compact denatured conformations, designated $D1$, $D2$, and $D3$, are shown in Table 1 and compared with the native state. The effective energies of the three denatured states are between 38 and 65 kcal/mol higher than that of the native state. This is a reasonable difference, considering the experimental protein stability and the estimated change in conformational entropy [29]. The radius of gyration (R_g) of the denatured conformations is only 12–18% greater than that of the N state; this is in agreement with the experimental data cited in the introduction. Nevertheless, the root mean square deviation (RMSD) of all backbone atoms from the crystal structure and between the three denatured states is more than 10 Å; the RMSD of the native state simulation from the crystal structure is 1.46 Å. The 'hydrophobic collapse' from the extended state found in the MD simulations is accompanied by formation of a large number of protein–protein hydrogen bonds; the number of hydrogen bonds in the denatured forms is only slightly smaller than that in the native state but very few are native-like. Moreover, the three denatured conformations have almost no native contacts (pairs of atoms more than three residues apart in sequence that are within 4 Å from each other in the crystal structure [28]). $D1$ has one native hydrogen bond between the $\beta 4$ and $\beta 6$ strands (58N–50O) within 1.5 times the distance in the crystal structure, $D3$ has no native contacts, and $D2$ has the 13 CG2-51 CG1 hydrophobic contact within twice the native distance. Thus, the three structures correspond to a reasonable, though limited, sample of the denatured ensemble.

From the average calculated enthalpy at 280 and 320 K and Eq. (1), the partial molar heat capacity of the native protein is estimated to be 2.75 kcal/mol K. Of this, 1.725 kcal/mol K arises from internal interactions and the rest from solvation (see Table 2). Although the calculation is highly approximate, this estimate is in the range of the experimental results. The value for the full, untruncated CI2 (83 residues instead of 64 considered here) at 298 K is 3.18 kcal/mol K [1]. The internal contribution is quite close to the value calculated for BPTI at 300 K from normal mode calculations [35].

Most of the internal contributions to $\overline{C}_p$, come from the covalent interactions (1.425 out of 1.725 kcal/mol K); these correspond primarily to the harmonic terms in the potential function. The total heat capacity arises 52% from covalent contributions, 11% from non-bonded contributions (van der Waals and electrostatic) and 37% from the solvation term. However, the covalent contribution is likely to be overestimated because of the classical treatment (see Section 2).

Table 1
Characteristics of native and denatured conformations[a]

	N[b]	$D1$	$D2$	$D3$
Effective energy[c]	−1970	−1931	−1905	−1932
(-vdW, -elec, -solv)	(453, 1083, 607)	(411, 1074, 614)	(399, 1052, 626)	(389, 1083, 627)
R_g at 300 K	11.38	12.91	12.78	13.40
H-bonds	60	53	54	58
RMSD from crystal	1.46	13.41	12.96	11.8
RMSD from $D1$			10.85	13.88
RMSD from $D2$				12.11
R_g at 350 K	11.17	12.97	12.64	13.07

[a] Energies in kcal/mol, R_g and RMSD in Å; the RMSD refers to the backbone atoms while R_g includes all atoms.
[b] N is the native state after 200 ps of molecular dynamics simulation at 300 K.
[c] After 300 steps of energy minimization.

Table 2
Estimation of $\Delta_N^D \overline{C}_p$ for CI2 at 300 K[a]

	$\langle W \rangle$	$\langle Hss \rangle$	$\langle H_{ss}^{cov} \rangle$	$\langle H_{ss}^{nonb} \rangle$	$\langle \Delta H^{slv} \rangle$	$\langle H \rangle$	C_p		
							Tot	Int	Solv
N							2.75	1.725	1.025
280 K	−1467	−815	578	−1393	−909	−1724			
320 K	−1361	−746	635	−1381	−868	−1614			
$D1$							3.45	2.675	0.775
280 K	−1449	−805	592	−1397	−928	−1733			
320 K	−1320	−698	651	−1349	−897	−1595			
$D2$							3.2	1.775	1.425
280 K	−1423	−762	583	−1345	−948	−1710			
320 K	−1310	−691	652	−1343	−891	−1582			
$D3$							3.175	1.85	1.325
280 K	−1442	−779	581	−1360	−954	−1733			
320 K	−1331	−705	642	−1347	−901	−1606			
$\Delta_N{}^U C_p$				$N \rightarrow D1$			0.7	0.95	−0.25
$\Delta_N{}^U C_p$				$N \rightarrow D2$			0.45	0.05	0.4
$\Delta_N{}^U C_p$				$N \rightarrow D3$			0.425	0.125	0.3

[a]Average energies over the last 2 ps of a 20-ps MD simulation at the designated temperature. N is native, D is denatured. Energies in kcal/mol, heat capacities in kcal/mol K. W is the effective energy, H_{ss} the intramolecular energy, H_{ss}^{cov} the covalent contribution to H_{ss} (bonds, bond angles, dihedral, and improper dihedral angles), ΔH^{slv} the solvation enthalpy, H the total enthalpy.

The results for the denatured conformations are also shown in Table 2. $D1$ has a heat capacity of 3.45 kcal/mol K (2.675 from internal interactions), $D2$ of 3.2 kcal/mol K (1.775 from internal interactions), and $D3$ of 3.175 kcal/mol K (1.85 from internal interactions). Comparing Tables 1 and 2, we see that the solvation contribution is not simply related to R_g. The experimental value for denatured untruncated CI2 given by Makhatadze and Privalov [1] at 298 K is 4.04 kcal/mol K. This is in reasonable agreement with the calculated average value of 3.275 kcal/mol K for the truncated version of CI2, despite the highly approximate nature of the calculation.

The estimated heat capacity of unfolding, $\Delta_N^D \overline{C}_p$, varies considerably for the three models of the denatured state. The average value is 0.525 ± 0.15 kcal/mol K, compared to the experimental value of 0.789 kcal/mol K [46] obtained with the untruncated form of CI2. Although the disordered N-terminal segment of CI2 is expected to contribute to the absolute heat capacity of the native and denatured states, its contribution to $\Delta_N^D \overline{C}_p$ may be small. The underestimation of $\Delta_N^D \overline{C}_p$ may be due to deficiencies of the hydration model (for example the group additivity assumption), to the obviously limited sampling of the denatured state or to the neglect of transitions on a longer time scale (see above). Covalent contributions are approximately equal in the denatured and native conformations and thus do not make a significant contribution to the unfolding heat capacity, as expected [13,39]; see also Section 2. In the case of $D1$, the solvation contribution is found to be negative despite the fact that exposure of non-polar groups is higher in D. This is due to the contribution of the third term in Eq. (7), which is included implicitly in the MD simulation at different temperatures but has not been considered in previous analyses. For example, increase in temperature may increase the exposure of polar groups in the denatured state and thus decrease the solvation enthalpy difference between $D1$ and N. Indeed, for $D1$ the non-polar surface area increases by 7 Å^2 whereas the polar surface area increases by 127 Å^2 between the

280-K and 320-K simulations. If the solvation enthalpy at 320 K is calculated from the ensemble of conformations generated at 280 K, the solvation heat capacity of $D1$ [the second term in the RHS of Eq. (7)] is calculated to be 1.225 kcal/mol K instead of the 0.775 that results when the change in conformational distribution is taken into account.

The compactness of the denatured conformations does not change substantially between 300 and 350 K (Table 1). The reason is that, although conformational entropy tends to make them more expanded as the temperature increases, the solvation free energy of both polar and non-polar groups increases with temperature and tends to make the protein more compact (so that the groups are less exposed) as the temperature increases. The heat capacity results at 350 K are shown in Table 3. The heat capacity of the native state increases from 2.75 at 300 K to 3.2 kcal/mol K at 350 K. The value at 350 K given by Makhatadze and Privalov [1] is 3.47 kcal/mol K. Both the internal and solvation terms increase with temperature, although the increase in the solvation term is larger.

The heat capacities of the three denatured conformations behave differently with temperature. For $D1$, the heat capacity at 350 K is lower than that at 300 K, but for $D2$ and $D3$ it is higher than at 300 K. The difference in heat capacity between N and D is smaller than at 300 K. This is in qualitative agreement with experiment [1].

Experimental dissection of the thermodynamic quantities of unfolding into internal and solvation contributions would be very useful but is very difficult. Recently, an approach was developed for the estimation of a contribution to the protein configurational entropy change on denaturation based on the mobility of backbone NH vectors as determined from NMR [47,48]. From the temperature dependence of this entropy contribution, heat capacity information could be extracted [49]. It was found that the entropy associated with backbone NH bond vectors increases with temperature more for the unfolded than for native proteins. This means that there is significant con-

Table 3
Estimation of $\Delta_N^D \overline{C}_p$ for CI2 at 350 K[a]

	$\langle W \rangle$	$\langle H_{ss} \rangle$	$\langle H_{ss}{}^{cov} \rangle$	$\langle \Delta H^{slv} \rangle$	$\langle H \rangle$	C_p		
						Tot	Int	Solv
N						3.2	1.8	1.4
330 K	−1331	−723	653	−861	−1584			
370 K	−1221	−651	725	−805	−1456			
$D1$						3.275	2.525	0.75
330 K	−1297	−692	670	−870	−1562			
370 K	−1181	−591	723	−840	−1431			
$D2$						3.4	1.5	1.9
330 K	−1282	−669	659	−885	−1554			
370 K	−1177	−609	733	−809	−1418			
$D3$						3.5	2.65	0.85
330 K	−1293	−673	655	−889	−1562			
370 K	−1166	−567	719	−855	−1422			
$\Delta_N{}^U C_p$				$N \rightarrow D1$		0.075	0.725	−0.65
$\Delta_N{}^U C_p$				$N \rightarrow D2$		0.2	−0.3	0.5
$\Delta_N{}^U C_p$				$N \rightarrow D3$		0.3	0.85	−0.55

[a]Average energies over the last 2 ps of a 20-ps MD simulation at the designated temperature. N is native, D is denatured. Energies in kcal/mol, heat capacities in kcal/mol K. W is the effective energy, H_{ss} the intramolecular energy, H_{ss}^{cov} the covalent contribution to H_{ss} (bonds, bond angles, dihedral, and improper dihedral angles), ΔH^{slv} the solvation enthalpy, H the total enthalpy.

tribution to the heat capacity of unfolding from intraprotein interactions, in accord with the results obtained here.

Calculated stability curves based on the compact models and the extended chain are shown in Fig. 1. The stability curve obtained from the experimental thermodynamic data [46] is shown in the same figure. It exhibits a maximum at approximately 270 K. The calculated temperature dependence of the stability exhibits the correct qualitative features, such as a maximum around room temperature, although the results do not agree quantitatively with experiment, as expected for the model calculations done here. The calculations based on the compact models give changes in ΔG with temperature comparable to experiment, whereas the calculation based on the extended chain gives variations in ΔG that are significantly too large, because the calculated values of all terms in the RHS of Eq. (8) are too large. This supports the conclusion that compact conformations are more reasonable models for the thermally denatured state.

The maximum in ΔG near room temperature results from competition between the two temperature dependent terms in the present model: there is the conformational entropy term, $T\Delta S^{conf}$, which increasingly favors the D state as

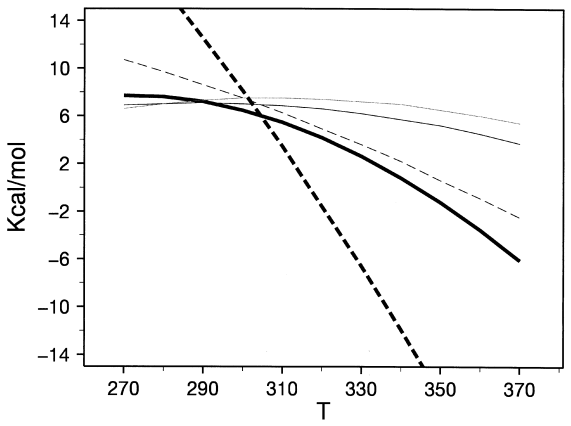

Fig. 1. Stability curves for CI2: experimental (thick solid line), based on $D1$ (thin solid line), based on $D2$ (thin dashed line), based on $D3$ (dotted line), and based on the extended chain (thick dashed line). The curves are fitted to the experimental value at 300 K (see text).

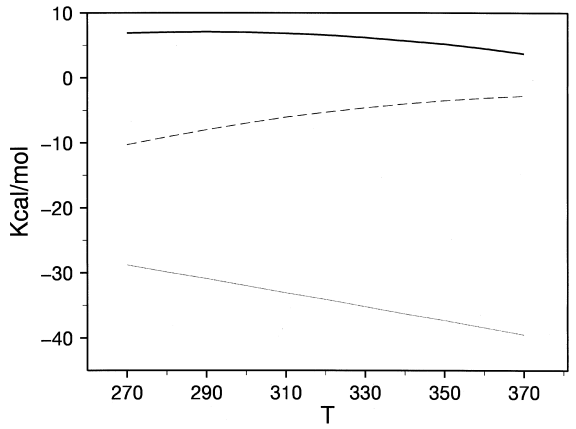

Fig. 2. Free energy of unfolding as a function of temperature (solid line), the conformational entropy contribution (dotted line), and the solvation free energy contribution (dashed line). These are based on the $D1$ model; the results for the other denatured conformations $D2$ and $D3$ are similar.

T increases, and the solvation term which increasingly favors the D state as T decreases (Fig. 2). Possible increases in ΔS^{conf} with temperature, which are neglected in the present calculations, would increase the curvature of the calculated stability curves and bring them in closer agreement with experiment. In terms of Eq. (8), denaturation is due to conformational entropy at high temperature and solvation free energy ($\Delta\langle\Delta G^{slv}\rangle$) at low temperatures. In $\Delta\langle\Delta G^{slv}\rangle$, the solvation free energy becomes less positive for non-polar groups and more negative for polar groups as temperature decreases. This makes exposure of non-polar groups less unfavorable and exposure of polar groups more favorable so that, as suggested by Makhatadze and Privalov [50], both polar and non-polar groups contribute to cold denaturation.

5. Conclusions

A method for estimating the heat capacity of proteins has been presented. The basis of the calculation is a model for the solvation free energy, enthalpy and heat capacity whose parameters were obtained from experimental data on the solvation of small molecules. This method differs from purely empirical approaches in that it does

not assume a fixed conformation for the denatured state but uses averages over conformations obtained from molecular dynamics simulations. Also, it includes the contribution from changes in the conformational distribution of the protein with temperature in the calculation of the heat capacity; this is neglected in other approaches. Although the calculation of the absolute partial molar heat capacities is highly approximate due to the use of classical mechanics, the results are of the correct order of magnitude. The heat capacity of unfolding should be less affected by the classical approximation.

The exposure of non-polar groups to water makes a large positive contribution to the heat capacity of unfolding in the present model, as well as in more empirical analyses. However, the results presented here suggest that a significant contribution to the heat capacity of denaturation comes from protein–protein non-bonded interactions. The denatured state is compact but more labile than the native state so that temperature can break interactions in D more easily than in N. This means that the enthalpy of D increases with temperature more than that of N and contributes significantly to $\Delta_N^D \overline{C}_p$. The same effect has been found to be important in lattice models for proteins that use temperature-independent interaction parameters [51]. The results demonstrate that relatively compact denatured states are consistent with the calorimetric data. The smaller contribution of hydrophobic group exposure to the heat capacity in this model for the denatured state is compensated by the contribution of non-covalent protein interactions.

The picture that emerges from the present study is considerably more complex than that derived from simple models that assume that all of the denaturation heat capacity arises from exposure of polar and non-polar surface area. It is reasonable that some correlation should exist between denaturation heat capacity and amount of buried non-polar surface area. However, this does not necessarily mean that all of this area will be fully exposed in the denatured state and suggests that the success of heat capacity calculations with simple surface accessibility models, which use a fully extended denatured state, may be fortuitous, in part.

The results presented here pertain to the thermally denatured state in the absence of denaturants and agree with experimental and simulation estimates concerning its compact nature. In solutions of urea or Gdn HCl, the solvation free energy of both polar and non-polar groups is more favorable [52] and a more expanded denatured state is expected.

Acknowledgements

This work was supported by a grant from the National Science Foundation and a Burroughs Wellcome PMMB postdoctoral fellowship to T.L. The authors are grateful to Benoit Roux for many insightful comments.

References

[1] G.I. Makhatadze, P.L. Privalov, Adv. Protein Chem. 47 (1995) 307.
[2] P.L. Privalov, E.I. Tiktopoulo, S.Y. Venyaminov, Y.V. Griko, G.I. Makhatadze, N.N. Khechinashvili, J. Mol. Biol. 205 (1989) 737.
[3] J.F. Brandts, J. Am. Chem. Soc. 86 (1964) 4302.
[4] J.M. Sturtevant, Proc. Natl. Acad. Sci. USA 74 (1977) 2236.
[5] R.L. Baldwin, Proc. Natl. Acad. Sci. USA 83 (1986) 8069.
[6] G.I. Makhatadze, P.L. Privalov, J. Mol. Biol. 213 (1990) 375.
[7] P.L. Privalov, G.I. Makhatadze, J. Mol. Biol. 224 (1992) 715.
[8] R.S. Spolar, J.-H. Ha, M.T. Record, Jr., Proc. Natl. Acad. Sci. USA 86 (1989) 8382.
[9] P.L. Privalov, S.J. Gill, Adv. Protein Chem. 39 (1988) 191.
[10] K.P. Murphy, S.J. Gill, J. Mol. Biol. 222 (1991) 699.
[11] R.S. Spolar, J.R. Livingstone, M.T. Record, Jr., Biochemistry 31 (1992) 3947.
[12] K.P. Murphy, E. Freire, Adv. Protein Chem. 43 (1992) 313.
[13] J. Gomez, V.J. Hilser, D. Xie, E. Freire, Proteins 22 (1995) 404.
[14] P. Calmettes, B. Roux, D. Durand, M. Desmadril, J.C. Smith, J. Mol. Biol. 231 (1993) 840.
[15] L.J. Smith, K.M. Fiebig, H. Schwalbe, C.M. Dobson, Folding Des. 1 (1996) R95.
[16] C. Tanford, Adv. Protein Sci. 23 (1968) 121.
[17] T.R. Sosnick, J. Trewhella, Biochemistry 31 (1992) 8329.

[18] A.M. Labhardt, J. Mol. Biol. 157 (1982) 331.
[19] S. Seshadri, K.A. Oberg, A.L. Fink, Biochemistry 33 (1994) 1351.
[20] A.D. Robertson, R.L. Baldwin, Biochemistry 30 (1991) 9907.
[21] O.B. Ptitsyn, Adv. Protein Sci. 47 (1995) 83.
[22] B. Nölting, R. Golbik, A.S. Soler-González, A.R. Fersht, Biochemistry 36 (1997) 9899.
[23] D. Shortle, FASEB J. 10 (1996) 27.
[24] D. Shortle, H.S. Chan, K.A. Dill, Protein Sci. 1 (1992) 201.
[25] E.E. Lattman, K.M. Fiebig, K.A. Dill, Biochemistry 33 (1994) 6158.
[26] C.J. Bond, K.-B. Wong, J. Clarke, A.R. Fersht, V. Daggett, Proc. Natl. Acad. Sci. USA 94 (1997) 13409.
[27] S.L. Kazmirsky, V. Daggett, J. Mol. Biol. 277 (1998) 487.
[28] T. Lazaridis, M. Karplus, Science 278 (1997) 1928.
[29] T. Lazaridis, M. Karplus, Proteins (1999) in press.
[30] P.L. Privalov, S.A. Potekhin, Methods Enzymol. 131 (1986) 4.
[31] S.J. Weiner, P.A. Kollman, D.T. Nguyen, D.A. Case, J. Comput. Chem. 7 (1986) 230.
[32] B.R. Brooks, R.E. Bruccoleri, B.D. Olafson, D.J. States, S. Swaminathan, M. Karplus, J. Comput. Chem. 4 (1983) 187.
[33] A. Ben-Naim, J. Phys. Chem. 82 (1978) 792.
[34] D.A. McQuarrie, Statistical Mechanics, Harper and Row, New York, 1976.
[35] B. Brooks, M. Karplus, Proc. Natl. Acad. Sci. USA 80 (1983) 6571.
[36] B. Tidor, M. Karplus, J. Mol. Biol. 238 (1994) 405.
[37] V. Volterra, Theory of Functionals, Dover, New York, 1930.
[38] F.H. Stillinger, T.A. Weber, Phys. Rev. A 25 (1982) 978.
[39] M. Karplus, T. Ichiye, B.M. Pettitt, Biophys. J. 52 (1987) 1083.
[40] O.M. Becker, M. Karplus, J. Chem. Phys. 106 (1997) 1495.
[41] T. Ichiye, M. Karplus, Proteins 11 (1991) 205.
[42] R.J. Petrella, T. Lazaridis, M. Karplus, Folding Des. 3 (1998) 353.
[43] P.L. Privalov, G.I. Makhatadze, J. Mol. Biol. 213 (1990) 385.
[44] E. Neria, S. Fischer, M. Karplus, J. Chem. Phys. 105 (1996) 1902.
[45] G.I. Makhatadze, P.L. Privalov, J. Mol. Biol. 232 (1993) 639.
[46] S.E. Jackson, A.R. Fersht, Biochemistry 30 (1991) 10428.
[47] M. Akke, R. Brüschweiler, A.G. Palmer, J. Am. Chem. Soc. 115 (1993) 9832.
[48] D. Yang, L.E. Kay, J. Mol. Biol. 263 (1996) 369.
[49] D. Yang, Y.-K. Mok, J.D. Forman-Kay, N.A. Farrow, L.E. Kay, J. Mol. Biol. 272 (1997) 790.
[50] P.L. Privalov, G.I. Makhatadze, J. Mol. Biol. 232 (1993) 660.
[51] A. Sali, E. Shakhnovich, M. Karplus, J. Mol. Biol. 235 (1994) 1614.
[52] C.N. Pace, CRC Crit. Rev. Biochem. 3 (1975) 1.